Stability and Postbuckling of a Platform with Flexible Legs Resting on a Slippery Surface

William I. Thacker
Computer Science Department
Winthrop University
Rock Hill, SC 29733

C.Y. Wang
Departments of Mathematics and Mechanical Engineering
Michigan State University
East Lansing, MI

Layne T. Watson
Departments of Computer Science and Mathematics
Virginia Polytechnic Institute and State University
Blacksburg, VA 24061-0106

ABSTRACT

A rigid platform is supported by thin elastic legs. The legs are able to slide on the ground as they deform. The governing equations for large deformations are formulated and solved numerically by homotopy and quasi-Newton methods. Nonlinear phenomena such as nonuniqueness are found. A global critical load for nonlinear stability is presented.

I INTRODUCTION

Flexible elements in structures are becoming important due to their light weight and resiliency. They are used in springs, linkages, robots and spacecraft. Due to the large nonlinear deformations involved, flexible elements are difficult to analyze theoretically [1–3]. Recently, Thacker et al. [4] studied a frame composed of a heavy platform supported by clamped-clamped flexible columns. It was found that, under finite disturbances, the structure buckles at a load well below the critical load determined by linear stability theory. This phenomenon is rare, but exists in some other instances such as the snap through of thin shells [5] or the buckling of a column with softening characteristics [6].

In this paper, we consider a loaded rigid platform supported by flexible legs and resting on a frictionless surface. The situation is equivalent to a table with wheels. We assume the table top is rigid and the firmly attached legs are elastic. The aim is to find the buckling load of the table under finite disturbances. This problem is similar to that of Thacker, et al. [4], but with the lower end of the legs free to move laterally instead of being clamped to the ground. The present model is applicable to more mobile structures such as carts and robots with legs.

We assume the load is symmetrically placed and the deformation is two dimensional. For example, if the platform is rectangular with four legs at the corners, the deformation would be in the plane of the two closest legs. We also assume the legs are uniform and flexible with negligible weight compared to the load. As we shall see later, the present results are quite different from previous results with clamped legs.

II FORMULATION

Fig. 1a shows the unbuckled state. The rigid platform is of length βL attached to legs of length L. The bottom ends of the legs have small wheels which can slide laterally. When the load is large enough, the legs may buckle as in Fig. 1b. We normalize all lengths by L and all forces by (flexural rigidity)$/L^2$. A Cartesian axis (x, y) is attached to the bottom of the left leg, which experiences a vertical reactive force of F_1. A moment balance on an elemental arc length ds (Fig. 1c) gives

$$dm + F_1 \sin\theta_1 ds = 0 \tag{1}$$

where θ_1 is the angle of inclination for the first (left) leg. But if the legs are thin, the Euler-Bernoulli law states

$$m = \frac{d\theta}{ds}. \tag{2}$$

Thus

$$\frac{d^2\theta_1}{ds_1^2} + F_1 \sin\theta_1 = 0. \tag{3}$$

Similarly, the governing equation for the second leg is

$$\frac{d^2\theta_2}{ds_2^2} + (F - F_1)\sin\theta_2 = 0. \tag{4}$$

The kinematic relations between arc lengths s_i and the coordinate axes are:

$$\begin{aligned} \frac{dx_1}{ds_1} &= \cos\theta_1, \\ \frac{dy_1}{ds_1} &= \sin\theta_1, \\ \frac{dx_2}{ds_2} &= \cos\theta_2, \\ \frac{dy_2}{ds_2} &= \sin\theta_2. \end{aligned} \tag{5}$$

The boundary conditions are that for $s_i = 0$ we are at the lower end of the legs so

$$x_1(0) = 0, \qquad x_2(0) = 0, \qquad y_1(0) = 0, \tag{6}$$

and the local moments there are zero:

$$\frac{d\theta_1}{ds_1}(0) = 0, \qquad \frac{d\theta_2}{ds_2}(0) = 0. \tag{7}$$

The fact the platform is rigid gives:

$$\begin{aligned} \theta_1(1) &= \theta_2(1), \\ \beta \cos\theta_1(1) &= y_2(1) - y_1(1), \\ \beta \sin\theta_1(1) &= x_1(1) - x_2(1). \end{aligned} \tag{8}$$

The last condition is the global balance of moment about the origin

$$(F - F_1) y_2(0) = F \left[y_1(1) + \frac{\beta}{2} \cos\theta_1(1) \right]. \tag{9}$$

Given F and β, there are nine boundary conditions for the nine unknowns: θ_1, θ_1', θ_2, θ_2', x_1, x_2, y_1, y_2, F_1.

It is true that Equations 3 and 4 have solutions in terms of elliptic functions. However, the angle θ is implicit in the elliptic integrals making the complicated boundary conditions, Equations (6-9), impossible to apply. Thus, we shall use the numerical method described below.

III NUMERICAL SOLUTION

A quasi-Newton based package MINPACK [8] and a homotopy based package HOMPACK [9] were used to solve the boundary value problem given by Equations (3–9). Note that the boundary conditions Equations (8–9) are highly nonlinear, so this is not a simple two-point boundary value problem. Let $\theta_1(s;X)$, $\theta_2(s;X)$, $x_1(s;X)$, $x_2(s;X)$, $y_1(s;X)$, $y_2(s;X)$ denote the solution to the initial value problem Equations (3–5) with fixed initial conditions Equations (6–7) and (unknown) initial conditions

$$X = \begin{pmatrix} \theta_1(0) \\ \theta_2(0) \\ y_2(0) \\ F_1 \end{pmatrix}. \tag{10}$$

The force F_1 is also unknown. Then the boundary value problem is equivalent to the nonlinear system of equations

$$H(X) = \begin{pmatrix} \theta_1(1;X) - \theta_2(1;X) \\ \beta \cos\theta_1(1;X) - y_2(1;X) + y_1(1;X) \\ \beta \sin\theta_1(1;X) - x_1(1;X) + x_2(1;X) \\ (F - F_1) y_2(0) - F \left[y_1(1;X) + \frac{\beta}{2} \cos\theta_1(1;X) \right] \end{pmatrix} = 0. \tag{11}$$

MINPACK would fail at times to converge to a solution because the starting guess for X was not "close enough" to the actual solution. This is a problem with all Newton and quasi-Newton method based solvers. The HOMPACK suite would then be employed since its convergence is global, i.e., a solution is found even if the starting point is not close to the solution. HOMPACK takes significantly more time (for this problem) to find a solution, and thus MINPACK would be tried first.

HOMPACK finds a solution by tracking the zero curve of $\lambda H(X) + (1-\lambda)(X-A)$ where A is the initial guess. As λ is increased from zero to one, the solution changes gradually from A to that of $H(X) = 0$. HOMPACK allows the zero curve to "turn back" on itself, making this a different and more robust method than standard continuation methods.

Typically, only the solution at the end of the zero curve (corresponding to $\lambda = 1$) is of interest. However, HOMPACK has an option for giving the zero curve itself. The parameter λ is usually not a physical parameter in the system to be solved. However, that is not a restriction. To find the displacement vs. F curves, F was replaced by $(1-\lambda)F_a + \lambda F_b$ such that when λ varied from 0 to 1, F varied over the interval $[F_a, F_b]$.

IV RESULTS AND DISCUSSION

As F is increased, we find three distinct modes of buckling described as follows. In Mode A, the platform remains horizontal at all times, with the legs symmetrically deformed. For Mode B, the platform becomes inclined. The distance between the ends of the legs is larger than the platform length. In Mode C, the platform becomes inclined, while the distance between the ends of the legs is smaller than the platform length.

The bifurcation of Mode A is the simplest. Since the platform remains horizontal, the deformations of each leg are similar to each other, and the vertical displacement will be independent of leg distance β. In this case, each leg is like a column, one end fixed and one end free with a compressive load $F/2$ [1, 7]. The buckling load is $\pi^2/2$. Fig. 2 shows the postbuckling shapes. Note that when $F > 6.802$ parts of the legs are below the horizontal, which cannot occur if the ground is solid. Therefore, we only attach physical significance to the cases where the legs are entirely above the horizontal. Fig. 3 shows the displacement of the center of the platform $\delta = 1 - \frac{1}{2}(x_1(1) + x_2(1))$ versus the total force F. The bifurcation from $\pi^2/2$ for Mode A is similar to that of column buckling. The dashed parts of the load-displacement curves in Fig. 3 show where some parts of the legs are below the horizontal. Since the legs are symmetric, Mode A configurations not only include the "spread out" case shown in Fig. 2, but also the case where both legs turn inwards.

Typical postbuckling shapes for Mode B are shown in Fig. 4. The bifurcation curves in Fig. 3 show Mode B is highly dependent on the length of the platform β. The slopes of the bifurcation curves are always positive. The initial bifurcation is at $\pi^2/2$ which is a side sway. Immediately, one leg collapses more and spreads out as shown in Fig. 4. As $\beta \to \infty$ Mode B does not approach Mode A where the platform remains horizontal. Of interest is the $\beta = 0$ case which represents two elastic legs clamped together at the top. After buckling (at $F = 19.2987$ instead of $\pi^2/2$) the legs spread apart as in Fig. 5. Since the slope of the bifurcation curve is positive, this buckled configuration is realizable as are all Mode B configurations.

Mode C is quite different. Since the legs bend inwards, the states are much less stable than Mode B. Fig. 6 shows that bifurcation starts at $\pi^2/2$, which is a side sway. Then, for $\beta < 530$, the slope of the bifurcation curve is negative at first, which is unrealizable. For $\beta < 1.301$, the slope is always negative and these states are always globally unstable. For $\beta > 1.301$, the value of F reaches a minimum. We call this minimum the global critical load F_{gc}, below which the system is stable (will return to its undeformed state) under all finite disturbances. Note that $F_{gc} = 0$ when $\beta < 1.301$. Fig. 7 shows F_{gc} for different β values. For large β, F_{gc} approaches $\pi^2/2$, which is the critical load for infinitesimal disturbances. Fig. 8 shows some buckled configurations in Mode C. Notice for $F = 4$ there are two unstable solutions, one realizable and one not, depending on whether the slope of the bifurcation curve is positive or negative.

Given β and F, we can conclude the following:

1. If $\beta < 1.301$ the frame always collapses when subjected to finite disturbances, even if the load is zero.
2. If $\beta > 1.301$ and $F < F_{gc}$ in Fig. 7, the frame is stable under any disturbance, infinitesimal or finite. If $\beta > 1.301$ and $F_{gc} < F < \pi^2/2$, the frame may have Mode C buckling.
3. If $F > \pi^2/2$ and $\beta \neq 0$, the frame is always unstable. Collapse is either in Mode A or Mode B. For these modes $F_{gc} = \pi^2/2$.
4. If $F > 19.299$ and $\beta = 0$, the frame is unstable under Mode B.

The least stable mode is Mode C, where the legs slide inwards, thus going to a narrower base from which to spring back. In order to increase stability, one should promote the legs spreading outwards, such as by adding constraints or slight initial inward curvature. Then the global stability criterion would be $F < \pi^2/2$.

We comment on the states corresponding to points on the dashed curves of Figs. 3 and 6. In the case when the ground is not penetrable, parts of the leg which may dip below the horizontal are then pressed up flat by the ground. Such a constraint increases stability and the actual curve would be to the right of the dashed curves. However, it would not alter the stability characteristics of states corresponding to points on the lower solid parts of the curves, whose study is the aim of the present paper.

The present work considers a platform supported by flexible legs with ends that can slide freely on the ground. In comparison to the situation where the legs are firmly clamped to the ground [4], we find significant differences. There exist three distinct postbuckling modes, while in the case of clamped-clamped legs there is only one mode. The global buckling load in the present case is much lower, and if the platform length is too short ($\beta < 1.301$), there is no safe load.

REFERENCES

1. R. Frisch-Fay, *Flexible Bars*, Butterworths, Washington D.C., 1962.
2. W. Gorski, A review of literature and bibliography on finite elastic deflections of bars, *Aust. Inst. Eng. Civil Eng. Trans.* CE 18: 74–85 (1976).
3. C. Y. Wang, A critical review of the heavy elastica, *Int. J. Mech. Sci.* 28: 549–559 (1986).
4. W. I. Thacker, C. Y. Wang, L. T. Watson, The nonlinear stability of a heavy rigid plate supported by flexible columns, *Int. J. Solids Struct.* 24: 3443–3449 (1993).
5. T. Von Karman, H. S. Tsien, The buckling of spherical shells by external pressure, *J. Aero. Sci.* 7: 43–50 (1939).
6. C. Y. Wang, Global buckling load of a nonlinearly elastic bar, *Acta Mech.* 119: 229–234 (1996).
7. S. P. Timoshenko, J. M. Gere, *Theory of Elastic Stability*, McGraw-Hill, New York, 1961.
8. J. J. Moré, B. S. Garbow, K. E. Hillstrom, *User Guide for MINPACK-1, ANL-80-74.* Argonne National Laboratory, Argonne, 1980.
9. L. T. Watson, M. Sosonkina, R. C. Melville, A. P. Morgan, H. F. Walker, HOMPACK90: A suite of FORTRAN 90 codes for globally convergent homotopy algorithms, *ACM Trans. Math. Software*, to appear.

Figure Captions

Fig. 1 (a) The unbuckled state, (b) the buckled state, (c) an element of a leg.

Fig. 2 Configurations of Mode A buckling, $\beta = 1$. (a) $F \leq \pi^2/2$, (b) $F = 5$, (c) $F = 6$, (d)$F = 6.802$.

Fig. 3 Displacement δ vs. F. Dashed curves show cases where legs are partially below horizontal. From left to right: Mode A, all β; Mode B, $\beta = 20, 5, 3, 2, 1, 0.5, 0.1, 0$.

Fig. 4 Configurations of Mode B buckling, $\beta = 1$, (a) $F \leq \pi^2/2$, (b) $F = 6$, (c) $F = 10$, (d) $F = 15$.

Fig. 5 Mode B buckling, $\beta = 0$, $F = 25$.

Fig. 6 Displacement δ vs. F, Mode C. Dashed curves show cases where legs are partially below horizontal. From left to right: $\beta = 0.5, 1.0, 1.3, 1.6, 2, 3, 5, 20, 50, 500$.

Fig. 7 Global critical load F_{gc} for Mode C.

Fig. 8 Configurations of Mode C buckling, $\beta = 3$. (a) $F \leq F_{gc} = 4.935$, (b) $F = 4.3$ (unstable) (c) $F = 4$ (unstable) (d) $F = 4$ (stable).

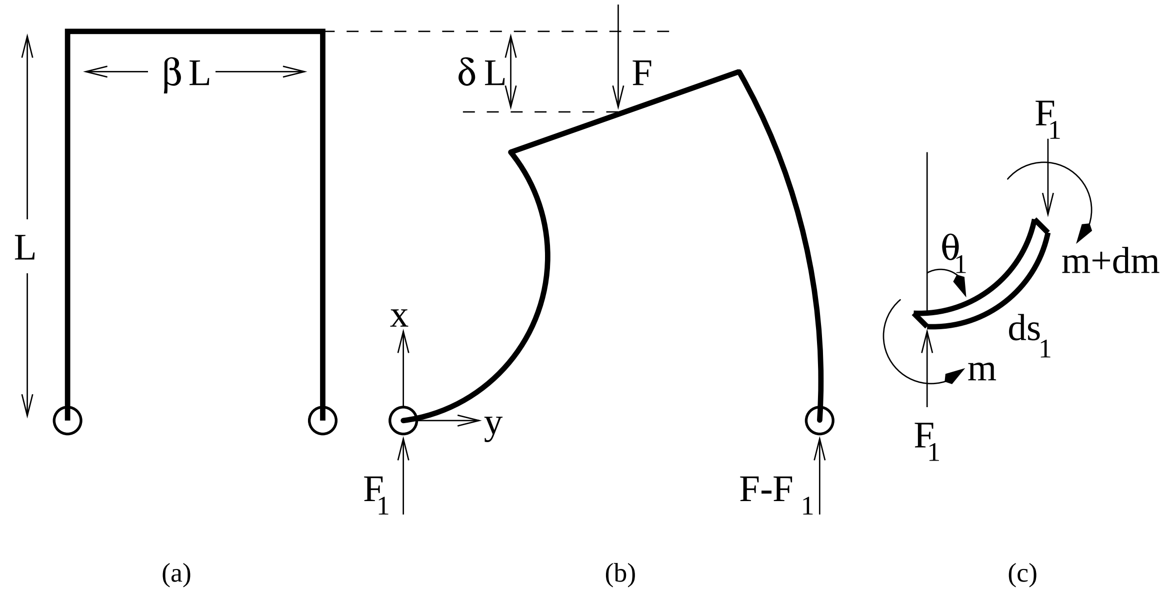

Fig. 1. (a) The unbuckled state, (b) the buckled state, (c) an element of a leg.

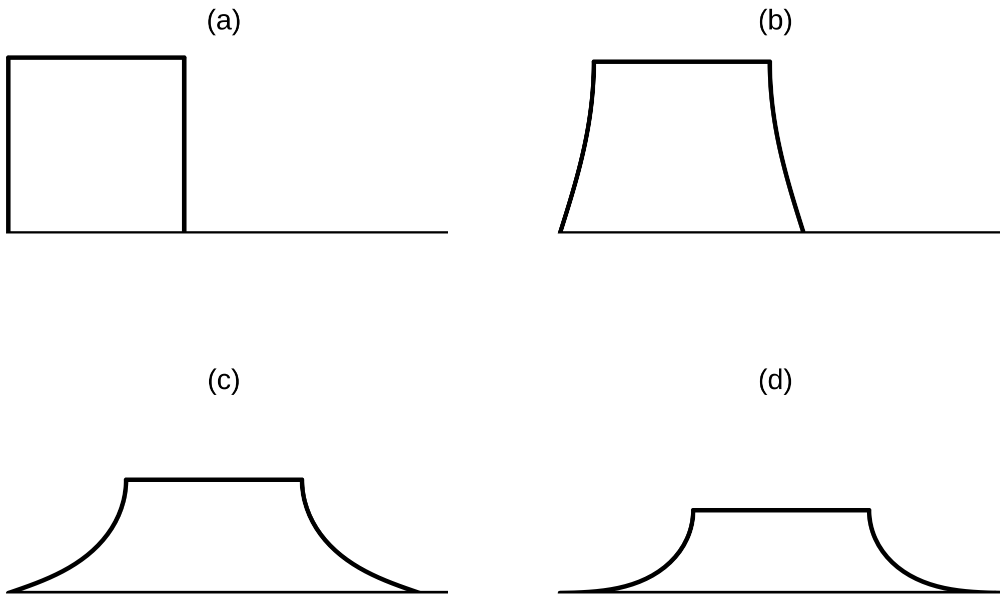

Fig. 2. Configurations of Mode A buckling, $\beta = 1$. (a) $F \leq \pi^2/2$, (b) $F = 5$, (c) $F = 6$, (d)$F = 6.802$.

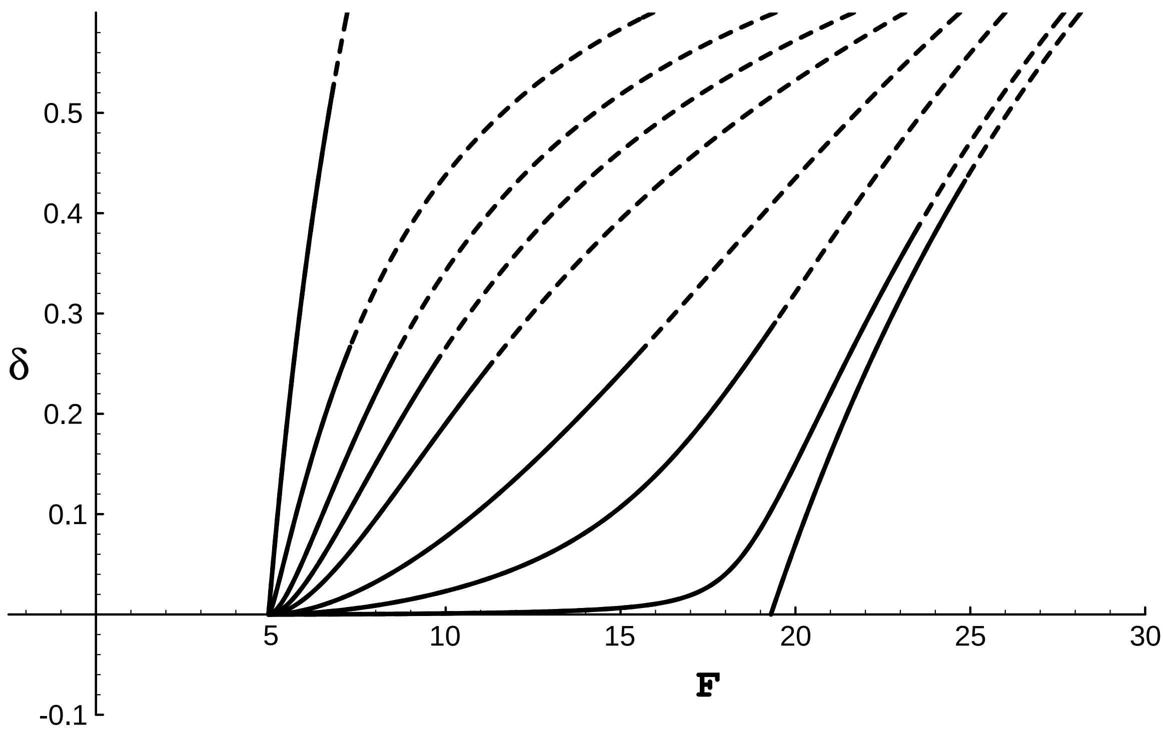

Fig. 3. Displacement δ vs. F. Dashed curves show cases where legs are partially below horizontal. From left to right: Mode A, all β; Mode B, $\beta = 20, 5, 3, 2, 1, 0.5, 0.1, 0$.

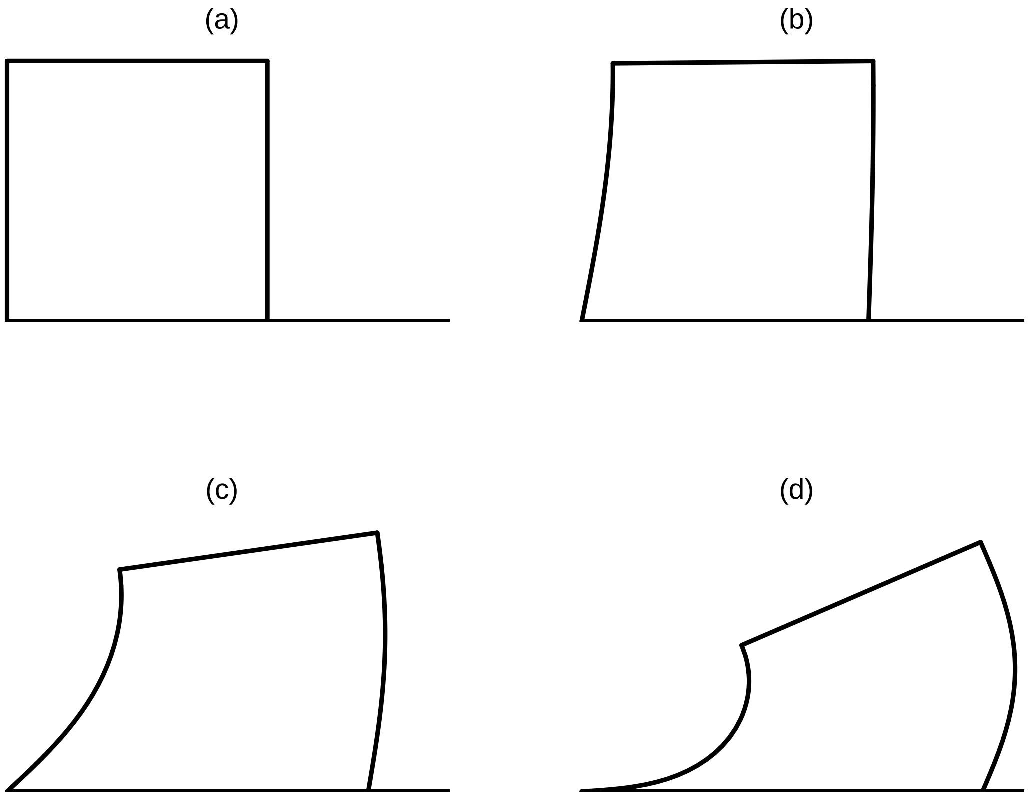

Fig. 4. Configurations of Mode B buckling, $\beta = 1$, (a) $F \leq \pi^2/2$, (b) $F = 6$, (c) $F = 10$, (d) $F = 15$.

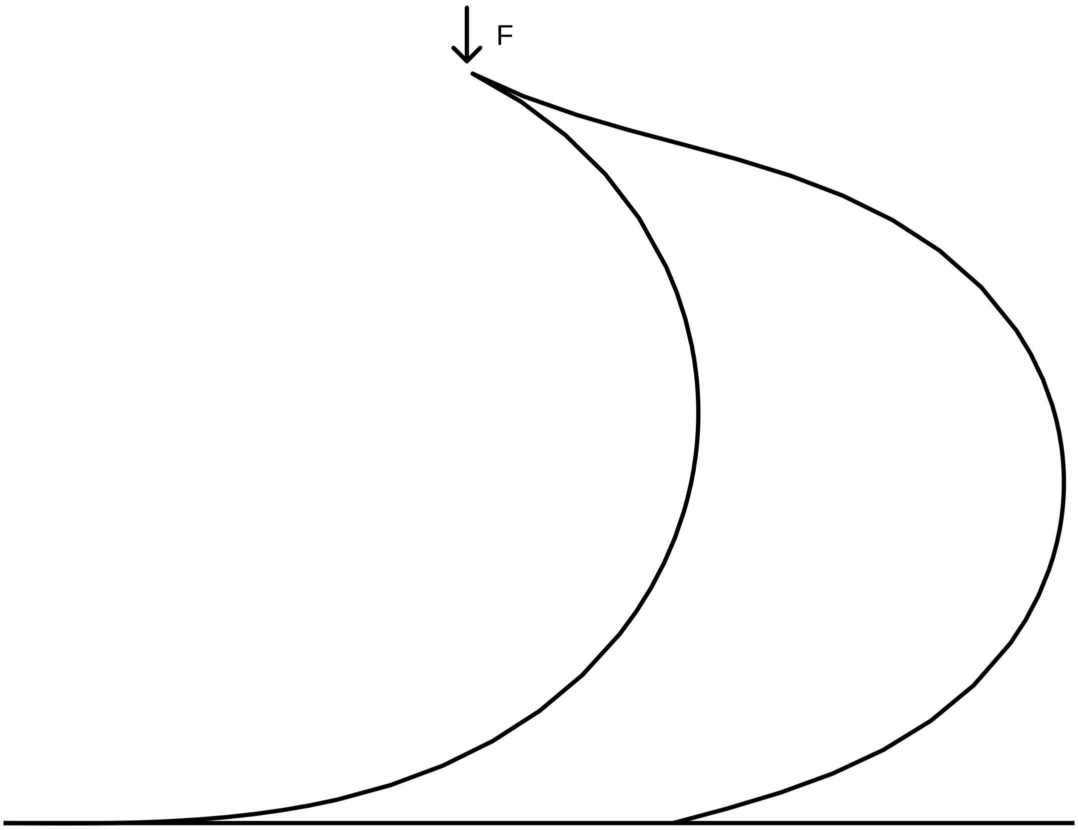

Fig. 5. Mode B buckling, $\beta = 0$, $F = 25$.

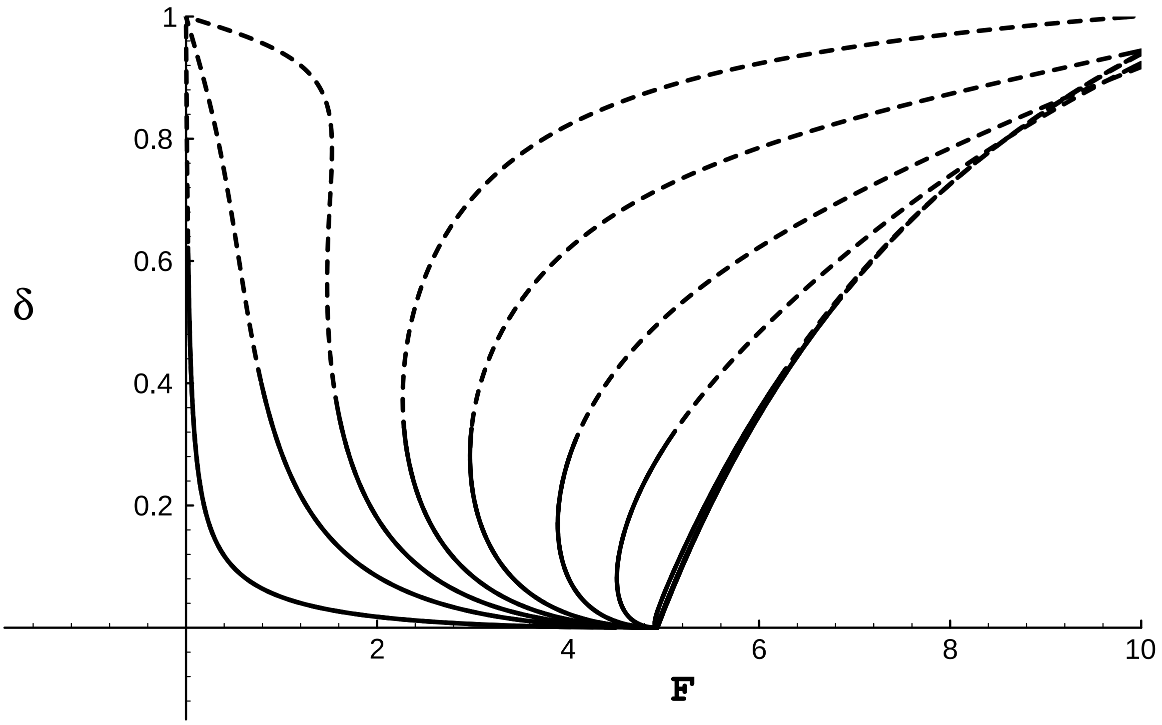

Fig. 6. Displacement δ vs. F, Mode C. Dashed curves show cases where legs are partially below horizontal. From left to right: $\beta = 0.5, 1.0, 1.3, 1.6, 2, 3, 5, 20, 50, 500$.

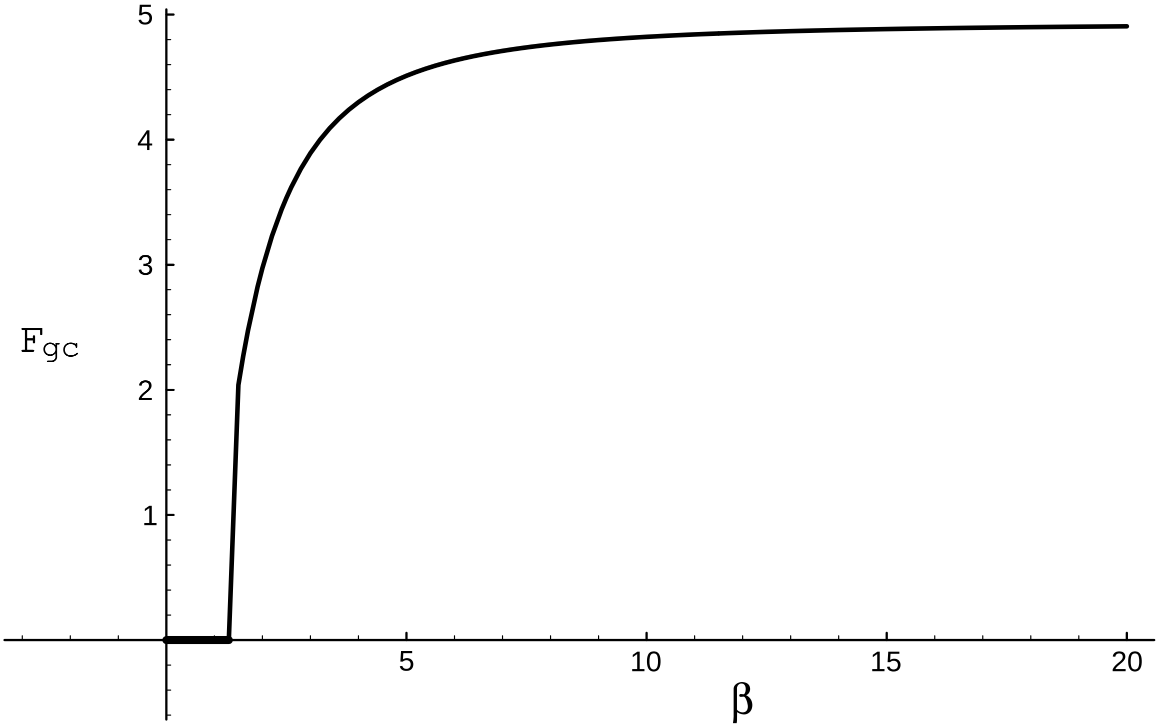

Fig. 7. Global critical load F_{gc} for Mode C.

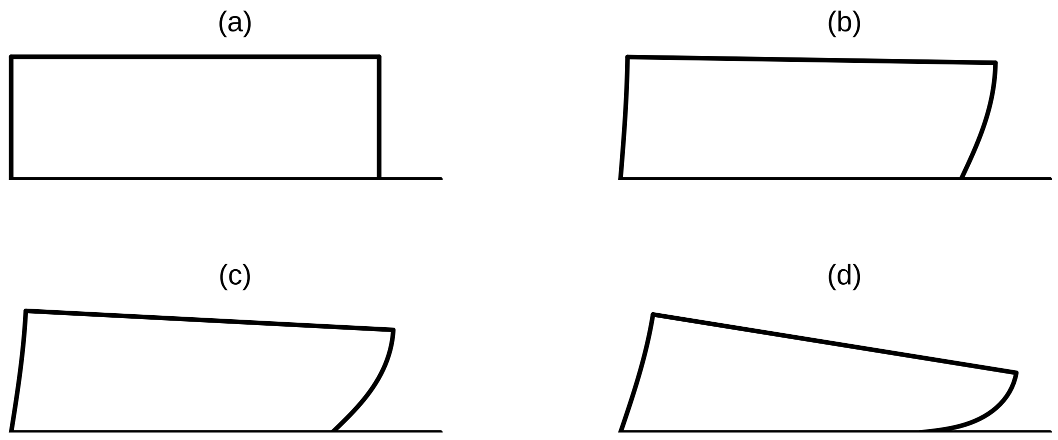

Fig. 8. Configurations of Mode C buckling, $\beta = 3$. (a) $F \leq F_{gc} = 4.935$, (b) $F = 4.3$ (unstable) (c) $F = 4$ (unstable) (d) $F = 4$ (stable).